New Journal of Physics
The open access journal for physics

High-field terahertz response of graphene

M J Paul[1], Y C Chang[2], Z J Thompson[1], A Stickel[1], J Wardini[1], H Choi[3], E D Minot[1], T B Norris[2,4] and Yun-Shik Lee[1]

[1] Department of Physics, Oregon State University, Corvallis, OR 97331, USA
[2] Center for Ultrafast Optical Science and Department of Electrical Engineering and Computer Science, University of Michigan, Ann Arbor, MI 48109, USA
[3] School of Electrical and Electronic Engineering, Yonsei University, Seoul, Republic of Korea
E-mail: tnorris@umich.edu

New Journal of Physics **15** (2013) 085019 (12pp)
Received 16 April 2013
Published 22 August 2013
Online at http://www.njp.org/
doi:10.1088/1367-2630/15/8/085019

Abstract. We investigate the response of multi-layer epitaxial graphene and chemical vapor deposition (CVD)-grown single-layer graphene to strong terahertz (THz) fields. Contrary to theoretical predictions of strong nonlinear response, the transmitted fields exhibit no harmonic generation, indicating that the nonlinear response is limited by fast electron thermalization due to carrier–carrier scattering. The fast electron heating gives rise to large THz transmission enhancement (>15%) in single-layer CVD graphene at high THz fields ($E_{\mathrm{THz}} > 10\,\mathrm{kV\,cm^{-1}}$). The nonlinear effects exhibit non-Drude behavior in the THz conductivity, where THz fields induce extreme non-equilibrium electron distributions.

[4] Author to whom any correspondence should be addressed.

Contents

1. Introduction

Graphene has attracted a great deal of attention from the scientific and industrial community since the initial demonstrations of isolated layers [1–4]. Among various applications, graphene is considered a promising electronic material for high speed electronic devices because of its high carrier mobility at room temperature and its high Fermi velocity ($\sim 1/300$ of the speed of light). Experimentally, high speed graphene devices such as 300 GHz transistors and photodetectors have been demonstrated [5–8]. As the operating frequency of graphene devices goes beyond 100 GHz, it becomes crucial to understand how this material behaves in the terahertz (THz) regime. In addition, due to many unique optical properties, such as strong THz absorption of one atomic layer [9] and plasmon resonances of patterned structures [10], graphene may play an important role in the so called THz gap (0.1–10 THz), where there is a need for improved sources and detectors. In a weak optical field where graphene behaves linearly, the optical properties have been studied extensively over a broad spectral range from visible to THz [11–13]. A universal optical conductivity of $\pi e^2/(2h)$ due to interband transitions is predicted and observed for photon energies less than ~ 1 eV and greater than twice the Fermi level E_F (Fermi level measured relative to the charge neutrality point) [11]. The optical conductivity of graphene demonstrates a Drude-like frequency dependence in THz frequency range [13–16].

Recent theoretical work on the high-field response of graphene indicates that the unique electronic properties of graphene lead to remarkably strong optical nonlinearities in the THz and IR regime [17–24]. The predicted strong nonlinear responses of graphene make it an attractive material for active photonic devices. Furthermore, as the internal electric field inside electronic devices could possibly reach 100 kV cm^{-1}, it is desirable to determine the maximum field at which graphene still behaves linearly. Transport in a strong field has also been studied theoretically, and nonlinear relationships between current and electric field are predicted [17–20]. Harmonic generation in graphene under a strong THz field has been predicted by several groups using different theoretical approaches [21–24]. For example, Mikhailov and Ziegler [21] analyzed the intraband contribution via the quasi-classical kinetic Boltzmann theory. In the limit of non-interaction quasi-particles, an electron gains a momentum $\mathbf{p}(t) = -\frac{e\mathbf{E}_0}{\omega_0}\sin\omega_0 t$ in an oscillating electric field $\mathbf{E}(t) = \mathbf{E}_0\cos\omega_0 t$. The electron moves in the same direction with $\mathbf{p}(t)$, yet its speed is constant, i.e. $v(t) = -v_F\,\mathrm{sgn}(\sin\omega_0 t)$. Accordingly, the sheet current density is expressed as $J(t) = -en_{2d}v(t) = en_{2d}v_F\,\mathrm{sgn}(\sin\omega_0 t)$, where n_{2d} is the sheet carrier density (see figure 1). This means that a sinusoidal excitation can produce a square wave-like current, and therefore odd harmonics are generated efficiently [21]. Wright *et al* [22]

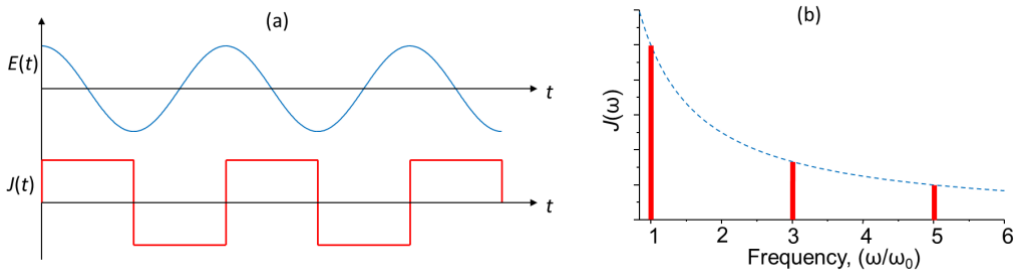

Figure 1. (a) Sheet current density in graphene induced by an oscillating electric field and (b) corresponding Fourier spectrum of the current density.

calculated the three-photon process in intrinsic graphene from the Dirac equation, and predicted a strong frequency-tripled current. Ishikawa [23] analyzed the THz harmonic generation from the Dirac equation by using a time domain approach. The threshold electric field to observe the nonlinear harmonic generation predicted by above works ranges approximately from 1 to 10 kV cm^{-1} [21–24], which is easily achievable in realistic devices, and in free-space THz spectroscopy.

It is important to note that all scattering mechanisms in graphene are neglected in the theoretical works predicting harmonic generation [21–24]. In realistic graphene systems, nonlinear effects may be obscured by various scattering mechanisms. First of all, many-body Coulomb interactions in graphene are strong [25, 26]. Carrier dynamics in graphene are also susceptible to defects, substrate interface interactions, and its own three-dimensional ripples [27]. Rigorous experimental studies are desirable to investigate how the intrinsic and extrinsic scatterings affect the nonlinear THz responses of graphene. Currently there are only few experiments on the high THz-field response of graphene [9, 28, 29]. Experimental observation of THz harmonic generation in graphene has not yet been reported. Dragoman *et al* [30] observed harmonic generation from graphene in the millimeter wave range, but the generation efficiency was extremely low.

In this paper, we present two experimental investigations of the high THz field response of graphene. In the first set of experiments, we searched for nonlinear harmonic generation in n-type multi-layer epitaxial graphene excited by broadband THz pulses whose peak field amplitude reaches 40 kV cm^{-1}; no nonlinear response was observed, contrary to a number of theoretical predictions in the literature, indicating the role of strong electron scattering in high fields. A second series of experiments probed the response of p-type single-layer chemical vapor deposition (CVD) graphene in the presence of strong THz fields up to 70 kV cm^{-1}. These experiments showed that THz-induced transparency becomes observable when THz fields exceed a moderate amplitude of 10 kV cm^{-1}. The nonlinear absorption in doped layers can also be seen as a consequence of increased electron scattering rates at high carrier energy.

2. Interaction of strong terahertz (THz) pulses with multi-layer epitaxial graphene

Our measurements of multi-layer epitaxial graphene were designed to search for THz harmonic generation in graphene. Strong single-cycle THz pulses were produced by two-color ionization of air [31–34]. The resulting THz radiation was focused onto a graphene sample, and the spectrum of the transmitted THz radiation is obtained by a Michelson interferometer.

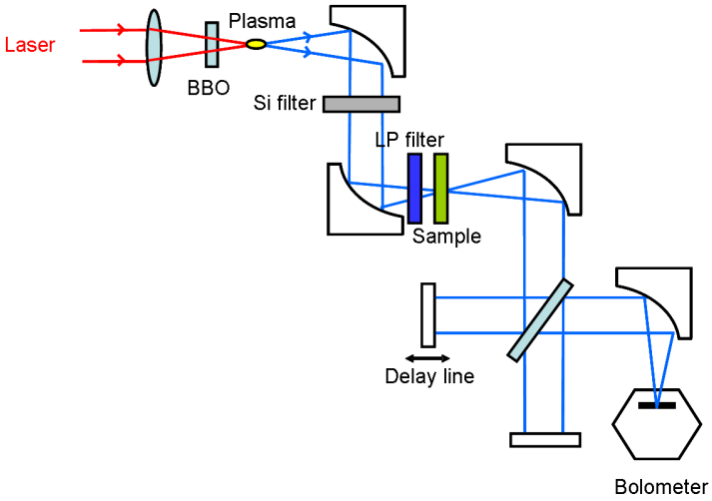

Figure 2. Schematic diagram of the experiment designed to search for THz nonlinear harmonic generation in graphene. Strong single-cycle THz pulses, produced by two-color ionization of air, are focused to a multi-layer epitaxial graphene sample. The spectrum is obtained by a Michelson interferometer and bolometer detection.

The optical setup is shown in figure 2. A 500 Hz regeneratively amplified Ti–sapphire laser system (lambda cubed laser system at University of Michigan) produces 30 fs, 3 mJ pulses [35]. The beam is focused by a lens, and a BBO crystal is placed between the lens and the focal point to generate second harmonic at 400 nm wavelength. The fundamental and second-harmonic pulses add coherently to produce a symmetry-broken field at the focus [31–34], which ionizes the air at the focal point. Because of the broken symmetry, the air plasma at the focal point contains a transient directional current [33, 34], which is the origin of THz radiation. THz radiation generated at the focal point is collimated and subsequently re-focused on the graphene sample by parabolic mirrors. A silicon low-pass filter blocks the unwanted optical light and a 3 THz low-pass filter (C103, IRLabs) further restricts the spectral range to below 3 THz. An epitaxial graphene sample is placed at the focal point of the second parabolic mirror. The sample has approximately ten graphene layers grown on C-face 4H-SiC substrate. The first few layers close to the SiC substrate are highly n-doped, while other layers are nearly intrinsic [36, 37]. The transmitted THz radiation is analyzed by a Michelson interferometer, in which the THz energy is measured by a bolometer (HD-3, IRLabs). By scanning the delay line of the Michelson interferometer, interferograms are acquired, and their Fourier transform gives the power spectra of the THz radiation [38]. The field strength at the focal point is 40 kV cm^{-1}, calculated from the measured pulse energy, duration and spot size.

Figure 3(a) shows the interferogram of the transmitted THz radiation, along with a reference interferogram acquired when the sample is not present. The transmission through this ten-layer epitaxial graphene sample is ∼50%, and the two interferograms are identical within the noise level when they are normalized, as shown in figure 3(b). This indicates that the graphene sample responds linearly to the incident THz field with a nearly flat spectral response. Figure 4 shows the transmission and reference spectra, calculated from the Fourier transform of the interferograms in figure 3. Most of the power of the incident THz radiation is below 3 THz

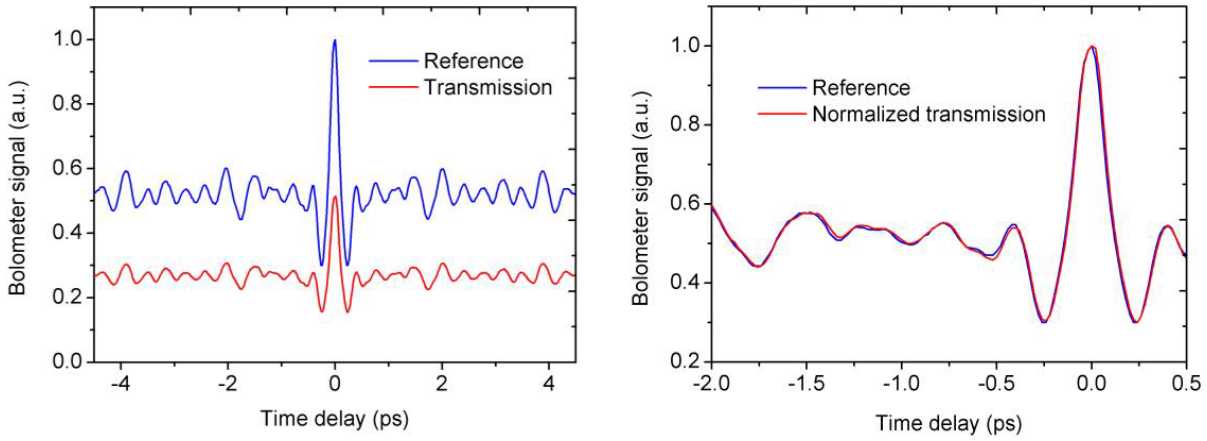

Figure 3. (a) The interferogram of the THz radiation that is transmitted through the graphene sample, and the reference interferogram acquired with the sample removed. (b) The same interferograms as (a) with their peaks normalized to the same value.

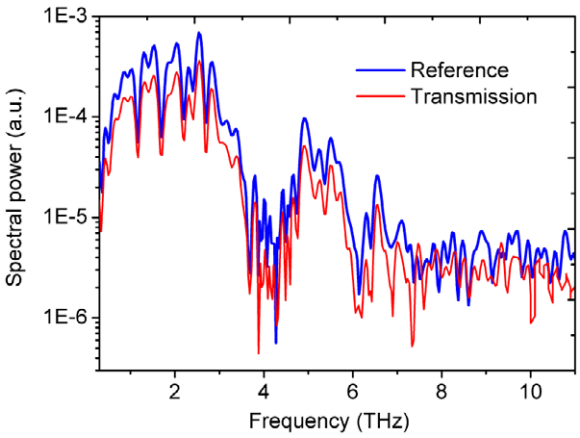

Figure 4. Reference and transmission power spectra obtained by the Fourier transform of the interferograms shown in figure 3(a).

because of the presence of the 3 THz low-pass filter. However, the transmission spectrum shows no increase of power above 3 THz. In the presence of noise and nonzero transmission through the low-pass filter above 3 THz, the minimal detectable third harmonic generation efficiency is ∼2%. The fact that the transmitted power is smaller than excitation power at all frequencies indicates that no nonlinear third harmonic generation larger than ∼2% is observed. We also vary the field strength by moving the graphene sample away from the focal point. Figure 5 shows that the normalized interferograms acquired from different field strengths are nearly identical, indicating lack of nonlinear harmonic generation.

These measurements show no observable THz harmonic generation in epitaxial graphene, even though the incident field greatly exceeds the predicted threshold field strength. The most likely explanation for the lack of nonlinear harmonic generation is the existence of fast carrier–carrier scattering when graphene is excited by a strong field [28]. Scattering mechanisms

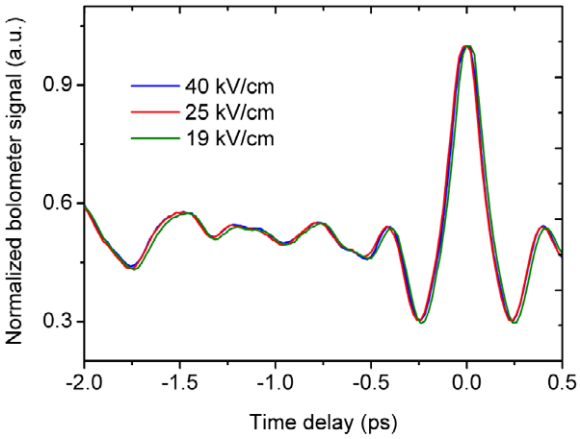

Figure 5. Normalized interferograms of the THz radiation transmitted through the graphene sample under different incident THz field strengths.

are neglected in the theoretical studies that predict harmonic generation [21–24], the justification being that the low-field mobility of electrons in graphene is very high [21]. However, in a strong field, electrons gain kinetic energy from the electric field, with an average energy much higher than the lattice thermal energy. Recent experiments and calculations [28, 39, 40] suggest that hot electrons in graphene undergo extremely fast carrier–carrier scattering, which becomes the dominant thermalization mechanism. Furthermore, unlike materials with parabolic bands, carrier–carrier scattering in graphene does not conserve current [39, 41]; in fact electron–electron scattering directly leads to damping of the current. When the electrons are energetically excited by the THz field, carrier–carrier scattering can occur in a time scale of $\sim$10 fs [28], much shorter than the THz pulse duration. Therefore, within the single-cycle THz pulse excitation, carrier-carrier scattering efficiently thermalizes the electrons and damps the current [28]. As a result the fast thermalization leads to a harmonic response of the entire electron gas to the applied THz field, suppressing any nonlinear harmonic generation [21]. Indeed, any theory of nonlinear response would have to include self-consistently the collective response of the electron gas to the applied field including current relaxation due to carrier scattering.

3. Nonlinear THz transmission spectroscopy of chemical vapor deposition-grown single-layer graphene

Unlike epitaxial multi-layer graphene, THz-induced nonlinear effects do become observable in CVD-grown single-layer graphene sheets when THz fields exceed a moderate amplitude, 10 kV cm^{-1}. We grew large-area, single-layer CVD graphene on Cu-foil via standard methods. Micro-Raman spectroscopy showed typical signatures of single-layer graphene [42]. The graphene layer had a p-type carrier concentration of $\sim 10^{12}$ cm^{-2}. The graphene sheet was subsequently covered with a thin poly(methyl methacrylate) (PMMA) layer (thickness $\sim$100 nm) and transferred to a sample holder that allows the graphene-on-PMMA film to be suspended freely over 2 mm diameter holes. The free-standing graphene–PMMA thin film sample structure reduces parasitic substrate effects in two ways: (i) THz absorption and interference caused by the substrate are negligible and (ii) the single graphene–PMMA interface

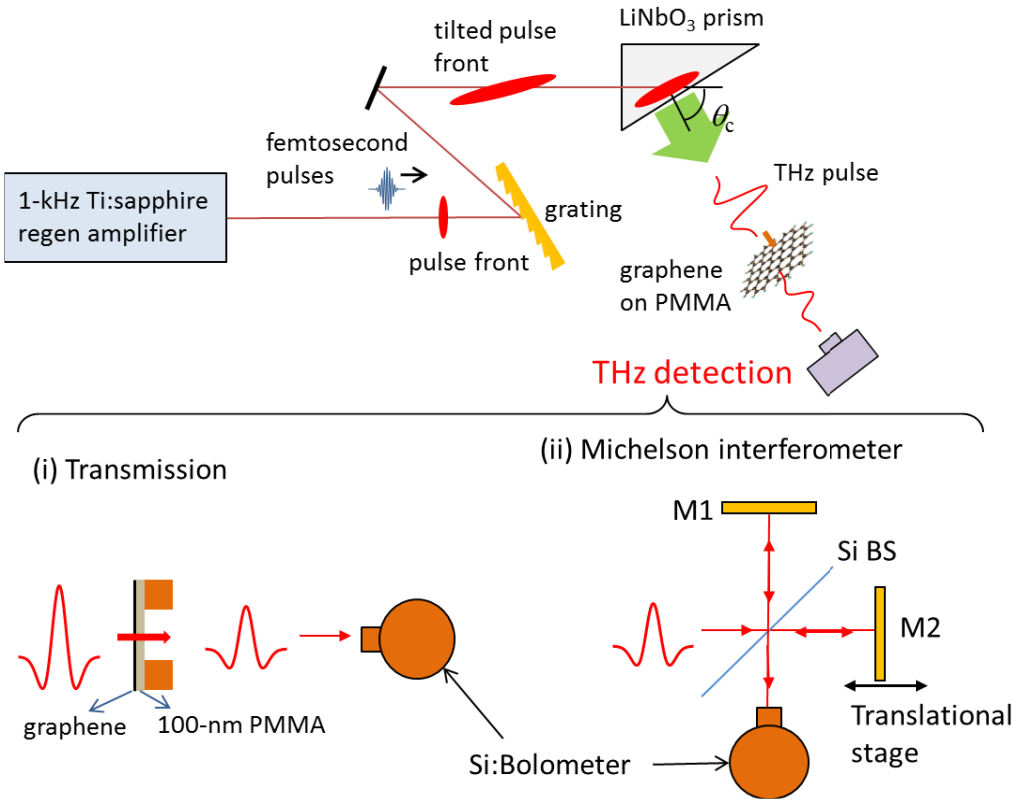

Figure 6. Schematic diagram of the nonlinear THz transmission measurements on CVD-grown single-layer graphene on a thin PMMA film. Strong broadband THz pulses are generated by tilted-pulse front optical rectification in $LiNbO_3$. Two THz detection schemes are employed: (i) spectrally integrated total THz transmitted power and (ii) transmission spectra via Michelson interferometry.

induces only small changes in the THz properties of graphene [16]. The PMMA is an uncharged polymer and contains much fewer charge traps than substrates like SiO_2.

We carried out THz transmission spectroscopy to investigate the frequency-dependent nonlinear response in the graphene samples. Strong, broadband THz pulses (central frequency, 0.9 THz; bandwidth, 0.6 THz) were generated by optical rectification of femtosecond laser pulses (pulse energy, 1 mJ; pulse duration, 90 fs; repetition rate, 1 kHz) with tilted pulse fronts in a $LiNbO_3$ crystal (THz field amplitude reaches 120 kV cm^{-1} at an optical pulse energy of 0.6 mJ) [43–45]. We detected the transmitted THz pulses using a liquid-He cooled Si:Bolometer to acquire (i) spectrally integrated total THz transmitted power and (ii) transmission spectra via Michelson interferometry as shown in figure 6.

Figure 7 shows power dependent measurements of spectrally integrated THz transmission through a free-standing graphene–PMMA layer. The large linear THz absorption by graphene (∼30%) at low intensities indicates that intraband transitions dominate the interactions of THz waves with graphene. From this, we obtained the sheet conductivity of the graphene sample ($\sigma_S \approx 1.0 \times 10^{-3}\ \Omega^{-1}$) using the thin-film transmission coefficient

$$t(\sigma_S) = \frac{2}{2 + Z_0\sigma_S}, \tag{1}$$

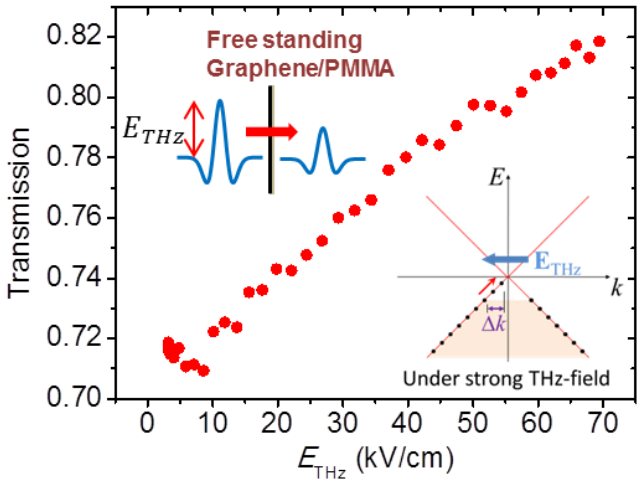

Figure 7. Strong THz fields enhance transparency in graphene: THz relative transmission versus field amplitude for a free-standing graphene–PMMA film.

based on the Drude model, where the graphene–PMMA layer was treated as an infinitely thin film [15, 16]. Z_0 (376.7 Ω) is the vacuum impedance. This simple picture, however, does not work at high THz intensities. The relative transmission through the graphene–PMMA film gradually increases for $E_{\mathrm{THz}} > 10\,\mathrm{kV\,cm^{-1}}$, and the transmission enhancement ($\Delta T/T$) reaches ∼15% at $70\,\mathrm{kV\,cm^{-1}}$. We speculate that strong THz pulses give rise to substantial changes in the electronic structure of graphene and the electron distribution via intraband transitions (inset of figure 7), and hence modulate the optical properties of the material.

The frequency-dependent THz transmission measurements shown in figure 8 provide more insights into the nonlinear THz effects. Figure 8(a) shows the interferograms of transmitted THz pulses when the peak THz fields are 5, 28, 47 and $59\,\mathrm{kV\,cm^{-1}}$. Figure 8(b) shows the Fourier spectra obtained from the interferogram at $59\,\mathrm{kV\,cm^{-1}}$. The frequency components above 2 THz are less than 0.5% compared to the peak at 0.9 THz. The result indicates that no harmonic generation larger than 0.5% is observed. The spectrum below 2 THz, however, shows small, yet noticeable changes as shown in the normalized transmission spectrum (figure 8(c)): we observed a slight blueshift relative to the reference spectrum ($\delta\nu = 0.07$ THz) while there is little change in the bandwidth (0.64 THz). The THz-induced spectral modulations correspond to the frequency-dependent transmission shown in figure 8(d), which were acquired by normalizing the Fourier spectra of the interferograms with the reference spectrum of no sample. The solid lines indicate linear fit for the spectra. The transmission enhancement at high THz fields is stronger at higher frequencies, while the flat transmission spectrum at the low field amplitude of $5\,\mathrm{kV\,cm^{-1}}$ is as expected from a Drude model at low THz intensities over this spectral range. The frequency-dependent transmission indicates that non-Drude behavior in the THz conductivity emerges at strong THz fields.

We performed an analysis of the THz-induced transparency using a simple phenomenological model based on energy-integrating saturable absorption:

$$I_T(t) = \frac{T_0 \exp[U_0(t)/U_{\mathrm{sat}}]}{1 + T_0\{\exp[U_0(t)/U_{\mathrm{sat}}] - 1\}} I_0(t), \tag{2}$$

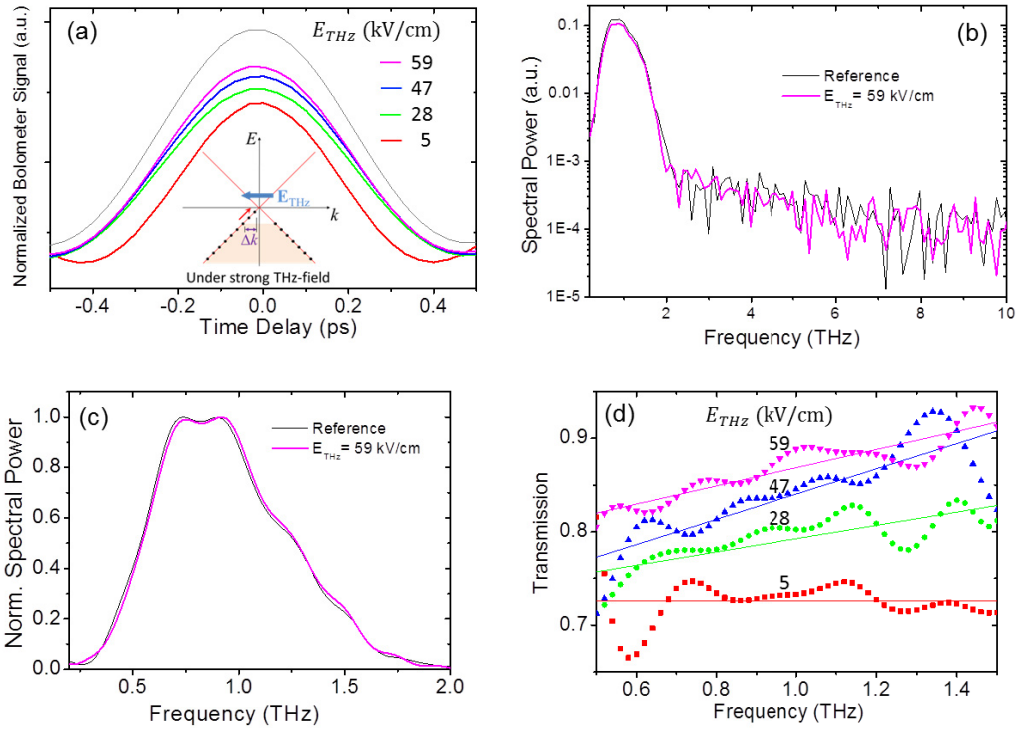

Figure 8. Nonlinear THz transmission of graphene measured by Michelson interferometer: (a) interferograms (the thin gray line indicates the interferogram of no sample), (b) power spectrum for $E_{\mathrm{THz}} = 59\,\mathrm{kV\,cm^{-1}}$, (c) normalized power spectrum for $E_{\mathrm{THz}} = 59\,\mathrm{kV\,cm^{-1}}$ and (d) transmission spectra and linear fits for $E_{\mathrm{THz}} = 5$, 28, 47 and $59\,\mathrm{kV\,cm^{-1}}$.

where T_0 is the linear transmission, U_{sat} is the saturation energy, $I_0(t)$ is the input pulse intensity at time t and $U_1(t) = \int_{-\infty}^{t} I_0(t)\,\mathrm{d}t$. The transient nature of saturable absorption gives rise to pulse shortening, which leads to a slight blueshift and spectral broadening. The results are, however, not quantitatively consistent with the experimental data. A full theoretical model including microscopic processes is required to fully understand the THz-induced transparency. Here we make a rough estimation how the strong THz fields induce nonlinear carrier dynamics in graphene. Strong THz pulses drive the electrons in graphene into a non-equilibrium state (inset of figure 8(a)), which transiently modulates the THz properties. With no THz-field present, the Fermi wavenumber k_{F} is roughly $10^6\,\mathrm{cm^{-1}}$ at a typical carrier density of the CVD graphene samples ($n \approx 10^{12}\,\mathrm{cm^{-2}}$). When the THz-driven electron momentum ($\Delta p = \hbar\Delta k$) exceeds the Fermi momentum ($p_{\mathrm{F}} = \hbar k_{\mathrm{F}}$), the electron transport will enter an extreme non-equilibrium regime. The gain of the electron momentum $\hbar\Delta k$ is approximately $eE_{\mathrm{THz}}\tau$, where τ is the scattering time. The far-from-equilibrium criterion, $\Delta k > k_{\mathrm{F}}$, is achieved in our experimental conditions of $E_{\mathrm{THz}} > 10\,\mathrm{kV\,cm^{-1}}$ with a typical scattering time $\tau \approx 10^{-13}\,\mathrm{s}$. The carrier acceleration and subsequent carrier–carrier scattering raise the electron temperature on a subpicosecond time scale. The temperature increase shortens the scattering time, which reduces conductivity, leading to the rise in transmission.

4. Conclusion

Strong-field THz spectroscopy has been applied to investigate the nonlinear carrier dynamics in graphene. Our preliminary studies show no harmonic generation in multi-layer epitaxial graphene or in p-type CVD-grown single-layer graphene, implying fast electron thermalization at subpicoseond timescales due to carrier–carrier scattering. The epitaxial graphene samples exhibit only linear THz responses up to amplitudes of $40\,\mathrm{kV\,cm^{-1}}$. Strong THz fields above $10\,\mathrm{kV\,cm^{-1}}$, however, enhance transparency of the CVD-grown graphene by heating the electrons and reducing the THz conductivity. We anticipate that these experiments will motivate the development of full theoretical models of carrier acceleration including strong fields and self-consistently accounting for carrier scattering.

Acknowledgments

The work at UM was supported by the NSF-MRSEC through contract DMR-0820382. The OSU work is supported by the National Science Foundation (DMR-1063632) and the National Research Foundation of Korea (NRF-2011-220-D00052). The work at Yonsei was supported by the National Research Foundation of Korea (NRF) grant funded by the Korean government (NRF-2011-220-D00052, no. 2011-0013255). We are grateful to Joshua Kevek for his expert advice.

References

[1] Novoselov K S, Geim A K, Morozov S V, Jiang D, Zhang Y, Dubonos S V, Grigorieva I V and Firsov A A 2004 Electric field effect in atomically thin carbon films *Science* **306** 666–9

[2] Novoselov K S, Geim K S, Morozov S V, Jiang D, Katsnelson M I, Grigorieva I V, Dubonos S V and Firsov A A 2005 Two-dimensional gas of massless Dirac fermions in graphene *Nature* **438** 197–200

[3] Geim A K and Novoselov K S 2007 The rise of graphene *Nature Mater.* **6** 183–91

[4] Castro Neto A H, Guinea F, Peres N M R, Novoselov K S and Geim A K 2009 The electronic properties of graphene *Rev. Mod. Phys.* **81** 109–62

[5] Lin Y M, Dimitrakopoulos D, Jenkins K A, Farmer D B, Chiu H-Y, Grill A and Avouris Ph 2010 100-GHz transistors from wafer-scale epitaxial graphene *Science* **327** 662

[6] Xia F, Mueller T, Lin Y M, Valdes-Garcia A and Avouris P 2009 Ultrafast graphene photodetector *Nature Nanotechnol.* **4** 839–43

[7] Vicarelli L, Vitiello M S, Coquillat D, Lombardo A, Ferrari A C, Knap W, Polini M, Pellegrini V and Tredicucci A 2012 Graphene field-effect transistors as room-temperature terahertz detectors *Nature Mater.* **11** 865–71

[8] Zheng J, Wang L, Quhe R, Liu Q, Li H, Yu D, Mei W N, Shi J, Gao Z and Lu J 2013 Sub-10 nm gate length graphene transistors: operating at terahertz frequencies with current saturation *Sci. Rep.* **3** 1314

[9] Hwang H Y, Brandt N C, Farhat H, Hsu A L, Kong J and Nelson K A 2011 Nonlinear THz conductivity dynamics in CVD-grown graphene arXiv:1101.4985 [cond-mat.mtrl-sci]

[10] Ju L *et al* 2001 Graphene plasmonics for tunable terahertz metamaterials 2011 *Nature Nanotechnol.* **6** 630–4

[11] Nair R R, Blake P, Grigorenko A N, Novoselov K S, Booth T J, Stauber T, Peres N M R and Geim A K 2008 Fine structure constant defines visual transparency of graphene *Science* **320** 1308

[12] Li Z Q, Henriksen E A, Jiang Z, Hao Z, Martin M C, Kim P, Stormer H L and Basov D N 2008 Dirac charge dynamics in graphene by infrared spectroscopy *Nature Phys.* **4** 532–5

[13] Horng J *et al* 2011 Drude conductivity of Dirac fermion in graphene *Phys. Rev.* B **83** 165113

[14] Choi H, Borondics F, Siegel D A, Zhou S Y, Martin M C, Lanzara A and Kaindl R A 2009 Broadband electromagnetic response and ultrafast dynamics of few-layer epitaxial graphene *Appl. Phys. Lett.* **94** 172102

[15] Tomaino J L, Jameson A D, Kevek J W, Paul M J, van der Zande A M, Barton R A, McEuen P L, Minot E D and Lee Y-S 2011 Terahertz imaging and time-domain spectroscopy of large-area single-layer graphene *Opt. Express* **19** 141–6

[16] Paul M J, Tomaino J L, Kevek J W, DeBorde T, Thompson Z J, Minot E D and Lee Y-S 2012 Terahertz imaging and time-domain spectroscopy of single-layer graphene embedded in dielectric media *Appl. Phys. Lett.* **101** 091109

[17] Bao W S, Liu S Y, Lei X L and Wang C M 2009 Nonlinear dc transport in graphene *J. Phys.: Condens. Matter* **21** 305302

[18] Dora B and Moessner R 2010 Nonlinear electric transport in graphene: quantum quench dynamics and the Schwinger mechanism *Phys. Rev.* B **81** 165431

[19] Mishchenko E G 2009 Dynamic conductivity in graphene beyond linear response *Phys. Rev. Lett.* **103** 246802

[20] Shishir R S, Ferry D K and Goodnick S M 2009 Room temperature velocity saturation in intrinsic graphene *J. Phys.: Conf. Ser.* **193** 012118

[21] Mikhailov S A and Ziegler K 2008 Nonlinear electromagnetic response of graphene: frequency multiplication and the self-consistent-field effects *J. Phys.: Condens. Matter* **20** 284204

[22] Wright A R, Xu X G, Cao J C and Zhang C 2009 Strong nonlinear optical response of graphene in the terahertz regime *App. Phys. Lett.* **95** 072101

[23] Ishikawa K L 2010 Nonlinear optical response of graphene in time domain *Phys. Rev.* B **82** 201402

[24] Shareef S, Ang Y S and Zhang C 2012 Room-temperature strong terahertz photon mixing in graphene *J. Opt. Soc. Am.* B **29** 274–9

[25] Bostwick A, Florian Speck S, Seyller T, Horn K, Polini M, Asgari R, MacDonald A H and Rotenberg E 2010 Observation of plasmarons in quasi-freestanding doped graphene *Science* **328** 999

[26] Chae J *et al* 2012 Renormalization of the graphene dispersion velocity determined from scanning tunneling spectroscopy *Phys. Rev. Lett.* **109** 116802

[27] Geim A K 2009 Graphene: status and prospects *Science* **324** 1530

[28] Tani S, Blanchard F and Tanaka K 2012 Ultrafast carrier dynamics in graphene under a high electric field *Phys. Rev. Lett.* **109** 166603

[29] Winner S *et al* 2012 Ultrafast carrier dynamics in graphene under a high electric field *Phys. Rev. Lett.* **107** 237401

[30] Dragoman M, Neculoiu D, Deligeorgis G, Konstantinidis G, Dragoman D, Cismaru A, Muller A A and Plana R 2010 Millimeter-wave generation via frequency multiplication in graphene *Appl. Phys. Lett.* **97** 093101

[31] Kim K Y, Taylor A J, Glownia J H and Rodriguez G 2008 Coherent control of terahertz supercontinuum generation in ultrafast laser–gas interactions *Nature Photon.* **2** 605–9

[32] Bartel T, Gaal P, Reimann K, Woerner M and Elsaesser T 2005 Generation of single-cycle THz transients with high electric-field amplitudes *Opt. Lett.* **30** 2805–7

[33] Kim K Y, Glownia J H, Taylor A J and Rodriguez G 2007 Terahertz emission from ultrafast ionizing air in symmetry-broken laser fields *Opt. Express* **15** 4577–84

[34] Karpowicz N, Lu X and Zhang X-C 2009 Terahertz gas photonics *J. Mod. Opt.* **56** 1137–50

[35] Hou B, Easter J, Mordovanakis A, Krushelnick K and Nees J A 2008 Vacuum-free x-ray source based on ultrafast laser irradiation of solids *Opt. Express* **16** 17695–705

[36] Sun D, Wu Z K, Divin C, Li X, Berger C, de Heer W A, First P N and Norris T B 2008 Ultrafast relaxation of excited Dirac fermions in epitaxial graphene using optical differential transmission spectroscopy *Phys. Rev. Lett.* **101** 157402

[37] Sun D, Divin C, Berger C, de Heer W A, First P N and Norris T B 2010 Spectroscopic measurement of interlayer screening in multilayer epitaxial graphene *Phys. Rev. Lett.* **104** 136802

[38] Bonvalet A and Joffre M 1998 Terahertz femtosecond pulses *Femtosecond Laser Pulses: Principles and Experiments* ed C Rulliere (Berlin: Springer) pp 309–31
[39] Sun D, Divin C, Mihnev M, Winzer T, Malic E, Knorr A, Sipe J E, Berger C, de Heer W A, First P N and Norris T B 2012 Current relaxation due to hot carrier scattering in graphene *New J. Phys.* **14** 105012
[40] Winzer T, Knorr A, Mittendorff M, Winnerl S, Lien M B, Sun D, Norris T B, Helm M and Malic E 2012 Absorption saturation in optically excited graphene *Appl. Phys. Lett.* **101** 221115
[41] Li X, Barry E A, Zavada J M, Buongiorno Nardelli M and Kim K W 2010 Influence of electron–electron scattering on transport characteristics in monolayer graphene *Appl. Phys. Lett.* **97** 082101
[42] Ferrari A C *et al* 2006 Raman spectrum of graphene and graphene layers *Phys. Rev. Lett.* **97** 187401
[43] Stepanov A G, Kuhl J, Kozma I Z, Riedle E, Almási G and Hebling J 2005 Scaling up the energy of THz pulses created by optical rectification *Opt. Express* **13** 5762–68
[44] Jewariya M, Nagai M and Tanaka K 2009 Enhancement of terahertz wave generation by cascaded $\chi^{(2)}$ processes in $LiNbO_3$ *J. Opt. Soc. Am.* B **26** A101–06
[45] Hirori H, Doi A, Blanchard F and Tanaka K 2011 Single-cycle terahertz pulses with amplitudes exceeding 1 MV cm^{-1} generated by optical rectification in $LiNbO_3$ *Appl. Phys. Lett.* **98** 091106